Degradation Behavior of Nanoreinforced Epoxy Systems Under Pulse Laser

M. Calhoun,[1] A. Kumar,[2] H. Aglan[1]

[1]*Mechanical Engineering Department, Tuskegee University, Tuskegee, Alabama 36088*
[2]*Physics Department, Tuskegee University, Tuskegee, Alabama 26088*

Received 9 September 2008; accepted 17 November 2008
DOI 10.1002/app.29887
Published online 7 May 2009 in Wiley InterScience (www.interscience.wiley.com).

ABSTRACT: Nanocomposites using EPON 824 as their matrix were exposed to pulse laser at 532 nm for various time intervals. The developed nanomaterials used for this study were manufactured using EPON 824 with multiwalled carbon nanotubes (MWCNTs) at a loading rate of 0.15% by weight and nanoclays at a loading rate of 2% by weight as reinforcements. The effect of laser irradiation on polymer composites has been investigated. The degradation mechanism for the epoxy was of a laser induced burning nature. Of all specimens tested, the ultimate strength of the MWCNT-reinforced specimens decreased the most as a function of radiation time; the nanoclay-reinforced epoxy retained the most strength after 2 min of laser radiation. In addition, the threshold fluence for decomposition indicated that less energy was required to initiate decomposition in the MWCNT-reinforced epoxy than in the nanoclay-reinforced epoxy. This can be attributed to the high thermal conductivity of the carbon nanotubes. Measurement of surface damage in the material was observed via electron microscopy. Fourier transform infrared spectroscopy was used to investigate changes to the molecular structure as a function of exposure time. © 2009 Wiley Periodicals, Inc. J Appl Polym Sci 113: 3156–3164, 2009

Key words: nanocomposites; mechanical properties; morphology; degradation; FTIR

INTRODUCTION

Durability of polymeric systems and their composites under various environmental conditions is a major concern for scientists and engineers, in that this ultimately determines the suitability of a material for specific applications. Understanding the degradation mechanisms for these systems under various challenging environmental conditions is extremely important in the determination of fatigue life. These environmental challenges include ultraviolet radiation, thermal events, moisture, corrosion, erosion among others.[1] Although there have been many studies reported in the literature concerning polymer degradation,[2–9] there has not been as much consideration toward investigating the degradation mechanisms of nanocomposites.

Polymers have been recognized for their use in improving material properties in specific applications, solar energy storage technology, and photosensitized reduction of water in microheterogeneous systems, photoelectrical systems, artificial photosynthesis, and spacecrafts.[10–17] It is well known that the performance of polymers degrades with continuous exposure to electromagnetic and solar radiation. The importance of this phenomenon is underscored in commercial and governmental sectors. Development of materials that are stable under extreme environmental conditions can significantly mitigate the huge costs associated with bridge and marine craft repair due to corrosion, road and structural repair due to repeated heat/cool cycles, as well as photodegradation of coatings on boats, aircrafts, and military vehicles. Ongoing development and testing of materials is critical toward this effort.

Carbon nanotubes and nanoclays have received considerable mention in recent years, each because of its own set of superior properties. Multiwalled carbon nanotubes (MWCNTs) can improve upon the thermal and mechanical properties of a polymer matrix. It has been well documented that MWCNTs have superior properties such as Young's modulus ($\leq$1 TPa), tensile strength (20–100 GPa), thermal conductivity [6000 W/(m K)], high aspect ratio, and specific strength (48.5 MN $\times$ m/kg), among others.[18] Ganguli et al.[19] studied the effect of loading rate and surface modification of MWCNTs on fracture toughness using a bifunctional epoxy as the polymer matrix. It was found that the addition of 0.15% MWCNTs, by weight, had an 80% improvement on

Correspondence to: H. Aglan (aglanh@tuskegee.edu).
Contract grant sponsor: US Department of Energy; contract grant number: DE-FG52-05NA27039.
Contract grant sponsor: National Science Foundation MRI Grant; contract grant number: CMS-0619827.

fracture toughness for that system. Likewise, it has been demonstrated that nanoclays in thermoset polymers can improve fracture toughness.[20,21] Smectic type clays, including montmorillonite, are attractive for use as fillers because of their lightweight nature. Their superior wetting abilities make them very promising in the field of barrier protection against corrosion.[22]

The degradation mechanisms of polymers which have been exposed to ultraviolet radiation (UV) have been examined. Aglan et al. examined the effect of UV radiation on polyurethane elastomers. It was found that discoloration appeared after only 1 month of exposure and that the tearing energy of the material decreased by 60% after 3 months and 98% after 5 months. DSC indicated a cleavage of the urethane bonds that was indicated by an increasing endothermic reaction with time.[23] In a companion study, Aglan and coworkers[24] confirmed the breakage of the urethane bonds facilitating aggregation between hard and soft segments in the molecular chains. Further, the increase in the melting enthalpy indicated an increase in this phase separation as a function of exposure time. Woo et al.[25,26] studied the effects of UV radiation on organoclayepoxy composites and found that the nanocomposite had shallower microcracks than the neat species after 300 h of exposure. In Additional, increasing the percentage of nanoclay lowered the tensile strength and strain to failure while increasing the modulus. This trend was unchanged as a function of UV radiation exposure, indicating that nanoclay loading rate, not UV radiation exposure, is the dominant factor in determining tensile strength. Even with accelerated UV test chambers, penetration of UV radiation, particularly through opaque materials, can be time consuming. Lasers can be used to study the degradation mechanism of these materials on a rapid time scale.

Laser radiation can interact with polymers via a variety of processes, depending on the frequency and power of the laser radiation and the energy band gap of the exposed material. If the polymer has an energy band which matches with the energy of an incoming photon, the light energy is absorbed. Generally, polymers will release absorbed energy as a nonradiative process, which leads to an increase in the temperature of the interaction zone, and finally, thermal damage in the neighborhood of the exposed area occurs. If the energy of the light is less than the energy band of the polymer, the light can be absorbed via a process called multiphoton absorption, followed by nonradiative relaxation and heating. However, the probability of multiphoton absorption is much less than of linear (single-photon) absorption. Another process called radiative ablation is almost independent of frequency of incoming photons, and it is caused by a strong electric field of photons sufficient to ionize atoms in the plasma state. This can be achieved by focusing the laser light at a spot on the top of the material. The average etch depth per pulse on a polymer surface exhibits a logarithmic dependence on the incident laser fluence (E) above a fluence threshold value (E_{th}) and is given by:

$$L_f = \frac{1}{\varepsilon_m} \ln \frac{E}{E_{th}}, \quad (1)$$

where ε is extinction coefficient (also called molar absorptivity in l mol/cm). The symbol m indicates molar concentration (mol/L). E is intensity of laser beam, and E_{th} is intensity threshold for onset of photodecomposition. The value of E_{th} can be obtained experimentally by plotting a graph between L_f and ln(E). Its intercept can give the value of ln E_{th}, and slope of the graph gives the value of $1/\varepsilon_m$.[27]

Possible mechanisms for etching vary between type of polymer and frequency of incident radiation. Perhaps the most likely mechanisms are the absorptions which promote thermal excitation in a sample, which means that the mechanism of etching from pulse to pulse can be different. The very first laser pulse may not create any etching in the sample, but it warms up and facilitates the burning and etching from the second pulse and onwards. In the present study, we used an unfocused laser beam from a frequency doubled YAG (neodymium-doped yttrium aluminum garnet; Nd:$Y_3Al_5O_{12}$) laser (532 nm), which is used to study the degradation of epoxy and epoxy nanocomposites by surrounding electromagnetic radiation on a rapid time scale. Neat EPON 824 and two nanoreinforcements, namely an organophilic layered silicate and MWCNTs, were exposed to the laser for 30 s, 1 or 2 min. The mechanical properties, fracture surface morphology, and changes in absorbencies as measured by Fourier transform infrared spectroscopy are reported.

MATERIALS

EPON 824

The structured epoxy resin used in this study was EPON 824, which was provided by Hexion Specialty Chemicals, Houston, TX. The epoxy resin is a high purity epichlorohydrin epoxy bisphenol A. The second part of the system is Epi-Cure 3277, which is a polyamide adduct in *n*-butanol.

Nanoclay

The nanoclay (NC) used for this study is a natural montmorillonite, which was provided by Southern Clay, Gonzales, TX. The nanoclay was modified with an ammonium salt to make it organophilic.

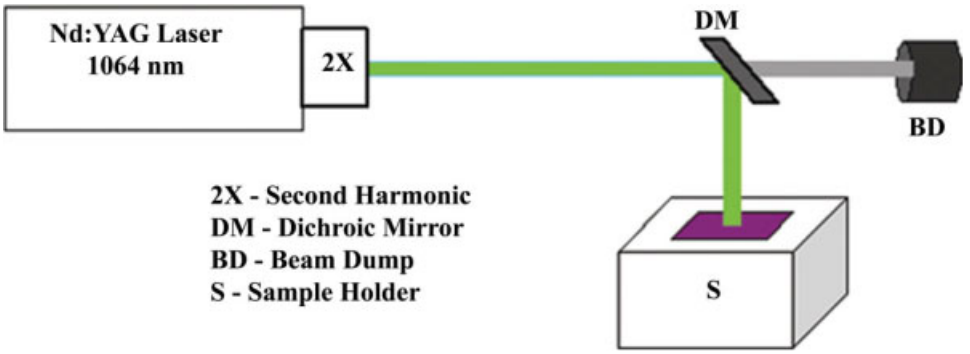

Figure 1 Schematic of Nd:YAG pulse laser setup. [Color figure can be viewed in the online issue, which is available at www.interscience.wiley.com.]

Multiwalled carbon nanotubes

MWCNTs were also used as nanoreinforcement for the epoxy system. The MWCNTs used in this study were provided by Ahwahnee Technologies, San Jose, CA. The diameter of these tubes was in the range of 2–15 nm, with a length of 1–10 μm, and 5–20 layers.

EXPERIMENTAL

Specimens were prepared in neat, 2% nanoclay, and 0.15% MWCNT formulations. The mix ratio used for resin to hardener was 2 : 1. All specimens were cured in an oven at 30°C for 16 h.

Nanoclay/EPON 824 nanocomposites

Nanoclay was added to the epoxy resin in small increments (10–15% of the total weight to be added) followed by mixing in a high shear mixer to remove agglomerates. Once all nanoclay was added to the resin, the mixture was left overnight to allow thorough wetting of the nanoparticles. After the hardener was added to the resin in the proper ratio, high shear mixing at 1800 rpm for three cycles of 30 s was used to ensure a well-dispersed system. The mixture was then poured into dogbone molds using a target of 3 mm thickness, and it was cured as previously described.

MWCNT/EPON 824 nanocomposites

The EPON 824 samples were also prepared in 0.15% MWCNT formulations by weight. A solution with an epoxy resin to MWCNTs ratio of 50 : 1 was prepared by high shear mixing. A 2% MWCNT/epoxy resin solution was prepared beforehand and diluted to achieve the desired 0.15% concentration. Samples were prepared as described above.

YAG pulse laser

This study employed a YAG (neodymium-doped yttrium aluminum garnet; Nd:$Y_3Al_5O_{12}$) laser. A schematic of the Nd: YAG laser setup is given in Figure 1. A dichroic mirror that reflects the 532 nm at 45° from the direction of the incident beam and transmits the residual first harmonic from the Nd:YAG laser was used to guide the 532 nm radiation (pulse duration $\sim$ 5 ns) onto the sample. The samples were exposed for the time durations of 30 s, 1 min, and 2 min. The average laser power used for exposing the samples was 2.6 W.

Tensile testing

The tensile strength of specimens was evaluated using a Sintec 5D Material Testing System. All specimens were tested at a crosshead speed of 12.7×10^{-5} m/s. The samples were dogbone shaped, with a gauge length of 88 mm, target thickness of 3 mm, and width of 12.7 mm at the most narrow point.

Microscopy

Fracture surfaces and crater morphology of epoxy samples were examined using a Hitachi S-2150 scanning electron microscope (SEM). Samples were observed at various magnifications with an accelerating voltage of 10 kV. Prior to being put into the vacuum chamber, samples were mounted with conductive tape and sputter coated with Au-Pd alloy. Optical micrographs were captured with a Wild Heerbrugg M3Z microscope.

Fourier transform infrared spectroscopy

Fourier transform infrared spectroscopy (FTIR) spectra were captured using a Nicolet 6700 FTIR spectrometer with an attenuated total reflectance (ATR) accessory. The FTIR spectrometer has a spectral resolution of 4 cm^{-1} over a 400–4000 cm^{-1} wavenumber range.

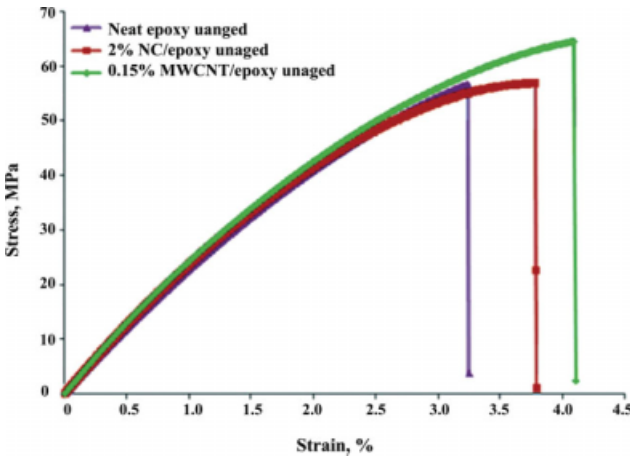

Figure 2 Stress–strain relationship of unaged neat and nano-reinforced epoxy. [Color figure can be viewed in the online issue, which is available at www.interscience.wiley.com.]

RESULTS AND DISCUSSION

Mechanical properties

All tensile tests were repeated a minimum of three times for each formulation and all exposure times. Representative specimens are reported. Figure 2 shows the stress–strain relationship of the unaged samples for the neat, 0.15% MWCNT/epoxy, and 2% nanoclay (NC)/epoxy nanocomposites. As can be seen in Figure 2, the ultimate strengths of the unaged specimens are approximately 59, 64, and 57 MPa for the neat epoxy, 0.15% MWCNT/epoxy, and 2% NC/epoxy nanocomposites, respectively. The addition of the MWCNT to the epoxy resin yielded a slight improvement in the ultimate strength over the neat epoxy, whereas the addition of the nanoclay resulted in a slight decrease in the ultimate strength in the epoxy nanocomposite. It should be noted, however, that this decrease is nominal and is not statistically significant (Table I). The strain to failure in both nanocomposite systems improved over the neat epoxy, and the 2% NC/epoxy formulation exhibits some plastic deformation, indicating an increase in ductility. It is seen from Figure 2, based on the first linear portion of the stress–strain behavior of the three materials, that there is no significant change in stiffness with such loadings of the nanoparticles.

Figure 3 shows neat and nanoreinforced epoxy after 2 min of laser radiation. The ultimate strength of the neat epoxy, 0.15% MWCNT/epoxy, and 2% NC/epoxy nanocomposites is 22, 17, and 40 MPa, respectively. The neat and 0.15% MWCNT/epoxy samples had significant loss in both ultimate strength and strain to failure after 2 min laser exposure as compared to the unaged specimens. The 2% NC/epoxy retained most of its ultimate strength with increasing exposure times, retaining almost 70% of its original ultimate strength after 2 min of laser radiation as compared to the unaged specimens. The neat epoxy retained about 40% of its original ultimate strength after 2 min exposure, whereas the 0.15% MWCNT/epoxy lost almost 75% of its original strength.

Table I shows the ultimate strengths for the three formulations at various time intervals of laser exposure. It can be seen that after 30 s, the ultimate strengths for the specimens were 52, 46, and 50 MPa for the neat epoxy, 0.15% MWCNT/epoxy, and 2% NC/epoxy nanocomposites, respectively. The neat epoxy and the 2% NC/epoxy nanocomposites both had a decrease in ultimate strength of about 7 MPa over their unaged formulations after 30 s of laser radiation. However, the 0.15% MWCNT/epoxy nanocomposite specimen had a decline of 18 MPa, representing a 28% decrease in ultimate strength over the unexposed specimens. It is clear that after only a short exposure to the laser, the 0.15% MWCNT/epoxy specimen lost a significant amount of its tensile strength. After 1 min, there was no significant difference in the ultimate strength of the 2% NC/epoxy specimen, whereas the ultimate strength of the neat epoxy and the 0.15% MWCNT/epoxy decreased by 23 and 50% over their unaged species, respectively. It is evident from this data that the nanoclay reinforcement enabled the epoxy to better resist loss in mechanical strength due to laser exposure.

Relationship between energy fluence and crater depth

After the nanoreinforced specimens were exposed to laser radiation for a period of time, craters were

TABLE I
Ultimate Strengths (MPa) of Neat and Nanostructured Epoxy Unexposed and After Various Pulse Laser Exposure Times

Formulation	Exposure			
	Unaged	30 s	1 min	2 min
Neat epoxy	57 ± 5.1	54 ± 3.2	44.2 ± 1.5	23.7 ± 5.4
2% NC/epoxy	56.1 ± 1.5	51 ± 4.0	54.2 ± 0.8	39.4 ± 6.0
0.15% MWCNT/epoxy	62.5 ± 2.9	48 ± 1.0	31.4 ± 1	15.9 ± 1.1

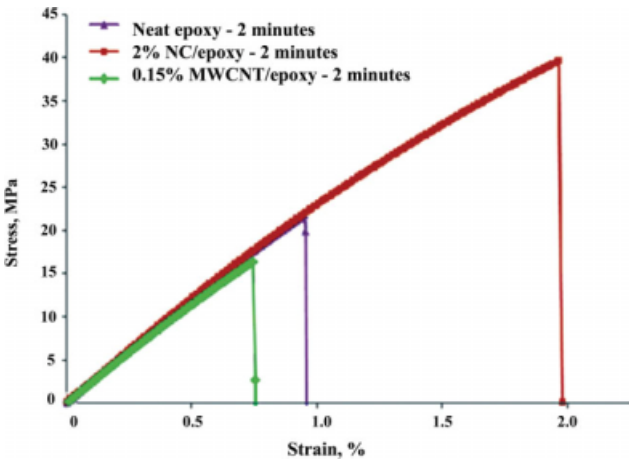

Figure 3 Stress–strain relationship of neat and nano-reinforced epoxy exposed to Nd:YAG Laser for 2 min. [Color figure can be viewed in the online issue, which is available at www.interscience.wiley.com.]

visible in them. It is believed that the nanoparticles created thermally active sites, thus creating craters at the laser exposed sites. The laser fluence in this study is above the threshold for ablation; hence, the crater formation is due to thermal decomposition (pyrolysis) and burning of the nanostructured epoxy by successive absorption of the laser pulse energy. Equation (1) was modified to fit our experimental conditions in order to determine the threshold fluence for thermal decomposition. The accumulative total energy was calculated as the product of total time of exposure and laser power. The maximum area of the exposed top surface was measured to be 6.35×10^{-5} m, based on the area of the laser. For each specimen type, the average etch depths were plotted against ln$E$, the energy fluence per unit area at 30, 60, and 120 s. The plot was fitted to a straight line, from which the fluence threshold was determined from the y-intercept of the plot. The results are shown in Table II. It was determined that the thresholds of accumulative laser fluence for decomposition in the 2% NC/epoxy and the 0.15% MWCNT/epoxy nanocomposites were 154.5 and 112.5 J/cm^2, respectively. This indicates that more accumulated energy was needed to begin decomposition in the 2% NC/epoxy nanocomposite than in the 0.15% MWCNT/epoxy nanocomposite. The difference in the fluence energies between the 2% NC/epoxy and the 0.15% MWCNT/epoxy can be attributed to the higher thermal conductivity of the MWCNT composite. This is based on our measurements of thermal conductivity of 5% by weight loading for both the MWCNT/epoxy and NC/epoxy nanocomposites, which revealed that the MWCNT/epoxy nanocomposite has a thermal conductivity of 0.27 W/(m K), whereas the NC/epoxy has a thermal conductivity of 0.197 W/(m K). The neat epoxy was also measured, and it was found to have a thermal conductivity of 0.194 W/(m K). The high thermal transport in carbon nanotubes is facilitated by the crystalline lattice structure of the nanotubes, comprised only of carbon atoms,[28] which offers multiple transport paths as compared to the amorphous structure of the epoxy matrix or the plate-like structure of the nanoclay. Thus the MWCNT/epoxy composite displays a higher capability for transporting heat than the nanosilicate composites.

TABLE II
Threshold Fluence for Decomposition of Nanostructured Epoxy

	2% NC/epoxy	0.15% MWCNT/epoxy
Threshold fluence (J/cm^2)	154.5	112.5

The depth of the craters formed in the materials as a result of laser radiation is shown in Table III. As can be seen in the table, crater formation in the 0.15% MWCNT/epoxy specimens occurred faster and was more pronounced than either the 2% NC/epoxy or the neat specimens. This data is in agreement with the fluence threshold data which suggests that less accumulated energy was required to begin thermal decomposition in the 0.15% MWCNT/epoxy than in the 2% NC/epoxy. As previously mentioned, MWCNTs have a robust thermal transport mechanism, which is evidenced by an average crater depth after 1 min of laser radiation of 0.48 ± 0.07 (15.24% penetration). The nanoclay loading rate used in this study is more than 10 times that of the MWCNT loading by weight, yet there was no sign of crater formation as a result of laser radiation in the 2%

TABLE III
Depth of Craters from Thermal Decomposition as a Result of Laser Exposure in Neat and Nanostructured Epoxy

	Neat epoxy			2% NC/epoxy			0.15% MWCNT/epoxy		
	30 s	1 min	2 min	30 s	1 min	2 min	30 s	1 min	2 min
Ave spl thickness (mm)	0.00	0.00	0.00	3.66 ± 0.17	3.37 ± 0.3	3.42 ± 0.21	3.25 ± 0.15	3.17 ±0.10	3.35 ± 0.24
Ave depth penetration (mm)	0.00	0.00	0.00	0.00	0.00	0.95 ± 0.05	0.11 ± 0.02	0.48 ± 0.07	1.13 ± 0.17
Penetration through sample (%)	0.00	0.00	0.00	0.00	0.00	27.99 ± 2.85	3.47 ± 0.4	15.24 ± 2.04	34.00 ± 7.22

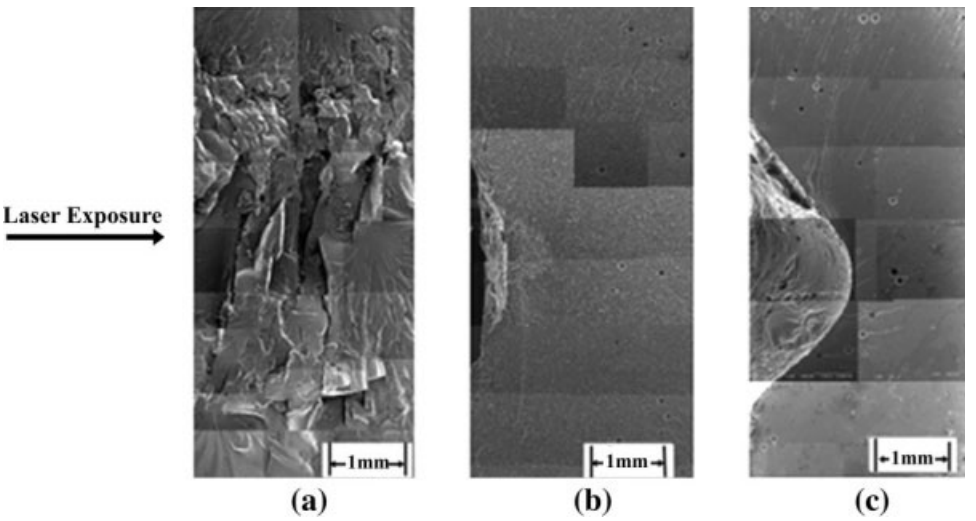

Figure 4 Composite fractographs of epoxy specimens exposed to Nd:YAG laser for 2 minutes at ×500 magnification: (a) neat EPON 824, (b) 2% NC/epoxy and (c) 0.15% MWCNT/epoxy.

NC/epoxy specimens after 2 min of exposure. This is due to the insulative properties of the nanoclay and the epoxy. For the neat specimens, however, it was apparent visually that the laser caused some internal damage. As the neat epoxy is transparent, the energy deposited on the sample from the laser permeated through the top layers and began to propagate, creating cracks and clefts in the interior of the specimens, which were seen at the fracture surface [Fig. 4(a)].

Composite fractographs for the neat epoxy, the 2% NC/epoxy, and the 0.15% MWCNT/epoxy are shown in Figure 4(a–c). As can be seen in Figure 4(a), there is severe internal damage to the specimen as a result of the laser exposure. The neat epoxy dissipated the laser energy throughout the material, creating an area characterized by cracks and roughness on the fracture surface. However, as the laser damaged the specimen prior to fracture, the features seen in the fractograph are indicative of the laser damage and not of resistance to fracture. Figure 4(b,c) show the fracture surface of the 2% NC/epoxy and the 0.15% MWCNT/epoxy after 2 min of laser radiation. There are craters present at the exposed areas because of laser radiation. The crater formations indicate that the laser damage was localized in the nanophase specimens. A rough area is observed just after the indentation in the 2% NC/epoxy specimen. This area just after the crater formation is indicative of the initial energy required to begin the fracture. This feature was not present in the 0.15% MWCNT/epoxy specimen and indicates that the MWCNT-reinforced specimen was less resistant to fracture than the NC-reinforced specimen. This correlates with the mechanical testing; the ultimate strength of the MWCNT-reinforced material decreased the most of all specimens tested as a function of duration of laser radiation.

Surface morphology

Optical and scanning electron micrographs showing the surface morphology at the laser exposed sites are seen in Figures 5 and 6, respectively. The micrographs in Figure 5(a–c) detail the laser spot at 6.5× magnification for the neat epoxy, 2% NC/epoxy,

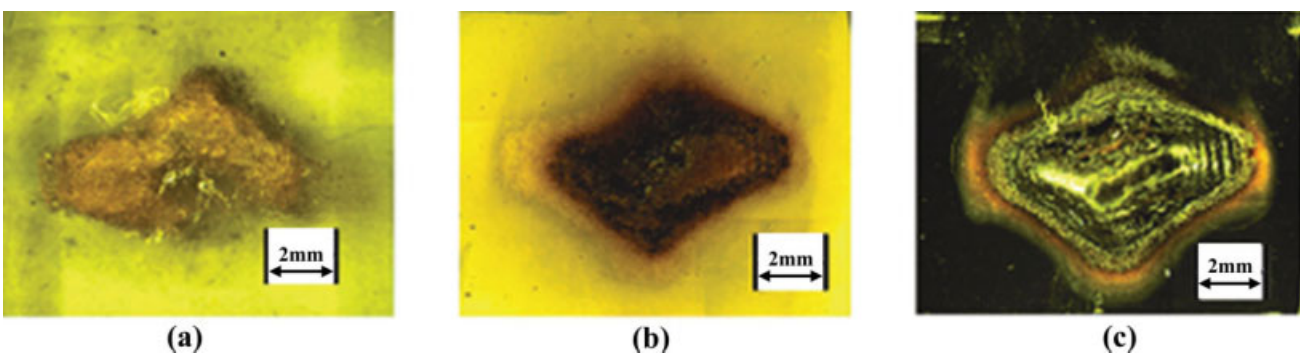

Figure 5 Optical microscope images of the laser damaged area of the (a) neat epoxy, (b) 2% NC/epoxy and (c) 0.15% MWCNT/epoxy. [Color figure can be viewed in the online issue, which is available at www.interscience.wiley.com.]

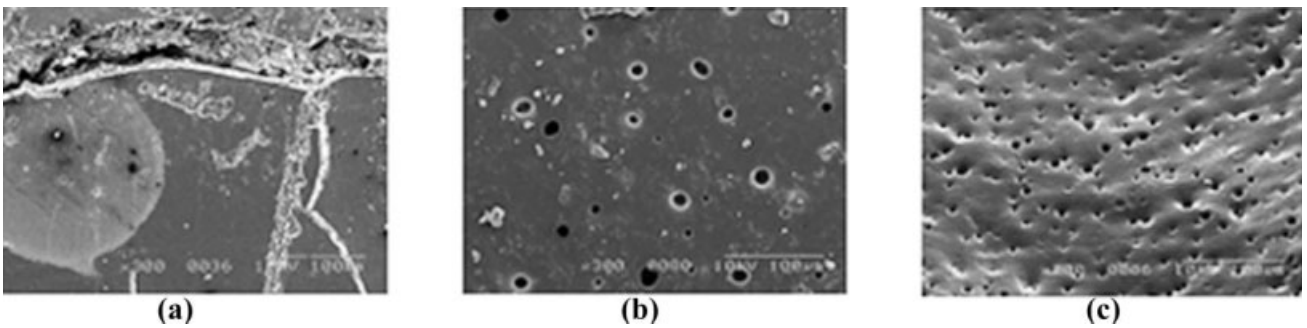

Figure 6 EM micrographs of 2 min laser exposed area at ×300: (a) neat epoxy, (b) 2% NC/epoxy and (c) 0.15% MWCNT/epoxy.

and 0.15% MWCNT/epoxy, respectively. As can be seen in Figure 5(a), there appears to be cracking just outside of the laser exposed area in the neat epoxy. This is consistent with the cracking seen in the fracture surface. There does not appear to be any charring on the laser exposed surface of the neat sample, whereas the 2% NC/epoxy and 0.15% MWCNT/epoxy [Fig. 5(b and c), respectively] do show evidence of charring. This is also consistent with the fracture surfaces, as etching occurred in the nanoreinforced specimens, forming craters. The area of the localized damage to the 0.15% MWCNT/epoxy samples is measurably larger than that of the 2% NC/epoxy samples.

Scanning electron micrographs at 300× are given in Figure 6(a–c), and they show the morphology of the laser exposed area of the neat epoxy, 2% NC/epoxy, and 0.15% MWCNT/epoxy, respectively. As expected, cracks are visible on the surface of the laser exposed area of the neat epoxy [Fig. 6(a)]. These cracks occurred as the neat epoxy absorbed energy given off by the laser. Given that epoxy is a crosslinked system, there was limited molecular mobility as the energy from the laser propagated through the specimens. In addition, there was no melting of the thermoset epoxy; hence, cracks formed in the material in order to dissipate the energy from the laser. Figure 6(b,c) shows the morphology of the area inside the craters formed by the laser for the 2% NC/epoxy and 0.15% MWCNT/epoxy, respectively. Pitting can be seen on the surface in both specimens. These pits range in size from $\sim$ 5 to 20 μm for the 2% NC/epoxy and $\sim$ 2–10 μm for the 0.15% MWCNT/epoxy. It is believed that these pits are the result of pyrolysis. It has been reported that MWCNT deposited on a thin silicon film exposed to Nd:YAG at 532 nm, can produce surface heat of as much as 1503°C in 13 ns.[29] The temperatures produced under sustained laser pulses are sufficient for pyrolysis to occur. The surface features seen in the nano reinforced specimens are likely to be due to gasses escaping from the matrix as it is softened by the laser radiation and the nanoparticles boring through the epoxy matrix.

FTIR analysis

FTIR spectra for the neat, 0.15% MWCNT/epoxy, and 2% NC/epoxy nanocomposites are shown in Figure 7(a–c). The spectra for all formulations show absorption bands at approximately the same wavenumbers for no exposure and 30 s and 2 min of laser exposure. It can also be seen in the figures that for the nanostructured formulations, the relative intensities of the major peaks decay as a function of exposure time to laser radiation. The amount of peak decay seen correlates with the threshold energies required for degradation of the specimens. Similar behavior has been previously reported for thermosetting polymer systems under CO_2 laser radiation.[30] Figure 7(b,c) shows representative spectra for the 0.15% MWCNT/epoxy and the 2% NC/epoxy at different exposure times. Peak decay correlating to CH_3 symmetrical bending in the bisphenol A structure is observed at 1378 and 1369 cm^{-1}. The primary aliphatic amine of the curing agent is observed at 1103 and 1089 cm^{-1}. The peak seen at 930 cm^{-1} corresponds to stretching of the C—O bonds. The degree to which we see peak decay is directly related to the threshold for decomposition in the polymers. Recall that the 2% NC/epoxy specimens had no measurable decomposition craters after 30 s of laser radiation, whereas the 0.15% MWCNT/epoxy had already begun to degrade after 30 s of exposure. This trend is also present in the FTIR spectra. The neat epoxy spectra show no signs of peak decay. There was a small peak that developed at 1548 cm^{-1}. It is believed this peak developed because of degradation products; however, further investigation is required to designate this peak.

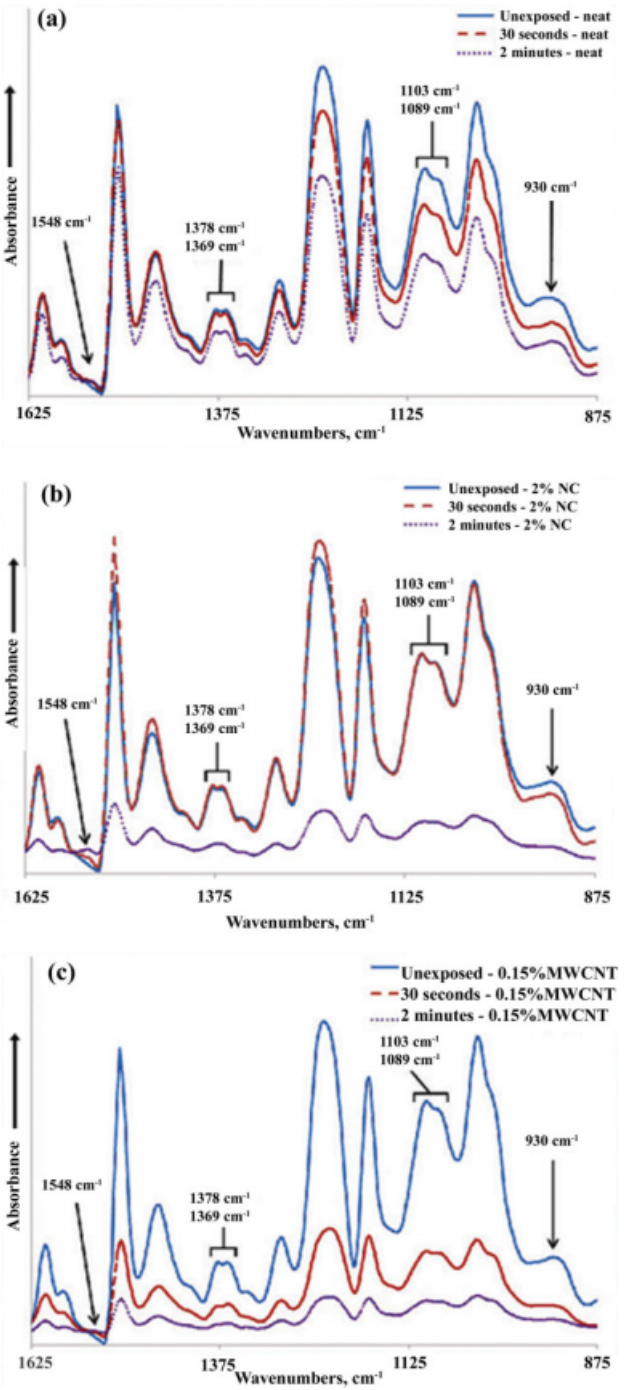

Figure 7 FTIR for unexposed, 30 s and 2 min laser exposure times: (a) neat epoxy, (b) 0.15% MWCNT/epoxy and (c) 2% NC/epoxy. [Color figure can be viewed in the online issue, which is available at www.interscience.wiley.com.]

CONCLUSIONS

- Neat EPON 824 epoxy and nanocomposites manufactured with MWCNTs and nanoclays were subjected to Nd:YAG laser radiation for different time intervals to study their degradation behavior. Prior to laser exposure, the ultimate strengths of the neat epoxy, 0.15% MWCNT/epoxy, and 2% NC/epoxy were 59, 64, and 57 MPa, respectively. After 2 min of exposure, the ultimate strengths of the neat epoxy, 0.15% MWCNT/epoxy, and 2% NC/epoxy had decreased to 23.7, 15.9, and 39.4 MPa, respectively.
- After exposure of only 30 s, both the neat and the 2% NC/epoxy showed no apparent damage, whereas the 0.15% MWCNT/epoxy had craters due to decomposition on its surface. The fracture surface of the three materials after 2 min showed that the neat epoxy had a crevice in the interior of the sample but no crater on the laser exposed side. The 2% NC/epoxy and the 0.15% MWCNT/epoxy specimens both had been etched from laser radiation; however, the indentations on the MWCNT-reinforced samples were much deeper and the fracture surface was much smoother than in the 2% NC/epoxy, indicating that the material was less resistant to fracture as a function of exposure time.
- The threshold fluence for laser decomposition was lower for the 0.15% MWCNT/epoxy than the 2% NC/epoxy; hence, less energy was required to decompose the MWCNT-reinforced material. This is attributed to the high thermal conductivity of the MWCNT, which accelerated pyrolysis in the nanocomposite.
- FTIR showed peak decay with respect to exposure time in the nanoreinforced polymers. The rate of peak decay correlates to the threshold fluence of decomposition. There was no peak decay observed in the neat epoxy.

References

1. Pandey, J. K.; Reddy, K. R.; Kumar, A. P.; Singh, R. P. Polym Degrad Stab 2005, 88, 234.
2. Pandey, J. K.; Singh, R. P. e-Polymers 2004, 51, 1.
3. Huaili, Q.; Chungui, Z.; Shimin, Z.; Guangming, C.; Mingshu, Y. Polym Degrad Stab 2003, 81, 497.
4. Morlat, S.; Mailhot, B.; Gonzalez, D.; Gardett, J. Chem Mater 2004, 16, 377.
5. Mailhot, B.; Morlat, S.; Gardett, J.; Boucard, S.; Duchet, J.; Gérard, J. Polym Degrad Stab 2003, 82, 163.
6. Sloan, J. M.; Patterson, P.; Hsieh, A. Polym Mater Sci Eng 2003, 88, 354.
7. Pramoda, K. P.; Liu, T.; Liu, Z.; He, C.; Sue, H.-J. Polym Degrad Stab 2003, 81, 47.
8. Du, J. X.; Wang, D. Y.; Wilkie, C. A.; Wang, J. Q. Polym Degrad Stab 2003, 79, 319.
9. Bourbigot, S.; Gilman, J. W.; Wilkie, C. A. Polym Degrad Stab 2004, 84, 483.
10. Klosterman, D.; Chartoff, R.; Graves, G.; Osborne, N.; Lightman, A.; Han, G.; Bezeredi, A.; Rodrigues, S. Ceram Eng Sci Proc 1998, 19, 291.

11. Lerch, B. A.; Draper, S. L.; Baaklini, G. Y.; Pereira, L. M. In HiTemp Rev 1999: Advanced High Temperature Engine Materials Technology Project; 1999; Vol. 2, p 30.
12. Gyekenyesi, A. L.; Baaklini, G. Y. In Proceedings from SPIE; Baaklini, G. Y.; Nove, C. A.; Boltz, E. S., Eds.; Bellingham, WA, 2000; Vol. 3585, p 142.
13. Gyekenyesi, A. L.; Baaklini, G. Y. In Proceedings from SPIE; Baaklini, G. Y.; Nove, C. A.; Boltz, E. S., Eds.; Bellingham, WA, 2000; Vol. 3993, p 78.
14. Abdul-Aziz, A.; Baaklini, G. Y.; Zagidulin, D.; Richard, W.; Rauser, R. W. In Proceedings from SPIE; Baaklini, G. Y.; Nove, C. A.; Boltz, E. S., Eds.; Bellingham, WA, 2000; Vol. 3993, p 35.
15. Li, J.; Tong, L.; Fang, Z.; Gu, A.; Xu, Z. Polym Degrad Stab 2006, 91, 2046.
16. Kashiwagi, T.; Grulke, E.; Hilding, J. Macromol Rapid Commun 2002, 23, 761.
17. Lie, D. L.; Mullan, C.; Favre, S.; O'Connor, G. M.; Glynn, T. J. Proceedings of the Third International WLT: Conference on Lasers in Manufacturing, Munich, Germany, June 2005.
18. Available at: http://www.Ahwahneetech.com. Accessed on June 9, 2008.
19. Ganguli, S.; Aglan, H.; Dennig, P.; Irvin, G. J Reinforced Plast Compos 2006, 25, 175.
20. Kim, B. C.; Park, S. W.; Lee, D. G. Comp Struct 2008, 86, 69.
21. Wang, L.; Wang, K.; Chen, L.; Zhang, Y.; He, C. Compos A 2006, 37, 1890.
22. Allie, L.; Thorn, J.; Aglan, H. J Appl Polym Sci 2008, 50, 2189.
23. Aglan, H.; Calhoun, M.; Allie, L. J Appl Polym Sci 2008, 108, 558.
24. Ludwick, A.; Aglan, H.; Abdalla, M. O.; Calhoun, M. J Appl Polym Sci 2008, 110, 712.
25. Woo, R. S. C.; Chen, Y.; Zhu, H.; Li, J.; Kim, J.; Leung, C. K. Y. Compos Sci Technol 2007, 67, 3448.
26. Woo, R. S. C.; Chen, Y.; Zhu, H.; Li, J.; Kim, J.; Leung, C. K. Y. Compos Sci Technol 2008, 68, 2149.
27. Rabek, J. F. In Photodegradation of Polymers: Physical Characteristics and Applications; Springer-Verlag: Heidelberg, 1996; Chapter 8.
28. Gojny, F. H.; Wichmann, M. H. G.; Fiedler, B.; Kinloch, I. A.; Bauhofer, W.; Windle, A. H.; Schulte, K. Polymer 2006, 47, 2036.
29. Nakamiya, T.; Ueda, T.; Ikegami, T.; Mitsugi, F.; Ebihara, K.; Tsuda, R. Diamond Relat Mater, to appear.
30. Bormashenko, E.; Pogreb, R.; Sheshnev, A.; Shulzinger, E.; Bormashenko, Y.; Sutovski, S.; Pogreb, Z.; Katzir, A. Polym Degrad Stab 2001, 72, 125.